RESEARCH ARTICLE

Taxon-specific C/N relative use efficiency for amino acids in an estuarine community

Xavier Mayali, Peter K. Weber & Jennifer Pett-Ridge

Chemical Science Division, Lawrence Livermore National Laboratory, Livermore, CA, USA

Correspondence: Xavier Mayali, Lawrence Livermore National Laboratory, 7000 East Ave, Livermore, CA, USA.
Tel.: +1 925 423 3892;
fax: +1 925 422 3160;
e-mail: mayali1@llnl.gov

Received 30 April 2012; revised 16 August 2012; accepted 18 August 2012.
Final version published online 20 September 2012.

DOI: 10.1111/j.1574-6941.12000.x

Editor: Tillmann Lueders

Keywords
nanosims; microarrays; microbial diversity; amino acid; biogeochemistry.

Abstract

Microbial activity plays a critical role in determining the nutrient status of an ecosystem (i.e. N or C limitation). While the balance of C/N assimilation has been measured at the whole community scale, quantitative detection of N and C assimilation from a single substrate at the scale of individual taxa has not been carried out. We recently developed Chip-SIP, a microarray and Nano-SIMS-based method for linking microbial phylogeny and function that allows simultaneous measurement of ^{15}N and ^{13}C incorporation. Here, we measured the relative incorporation of C and N from dual-labeled substrates by individual microbial taxa in bottle incubations of samples collected from an estuary. Incubation times < 24 h were sufficient to successfully detect active microbes incorporating ^{15}N ammonium. In subsequent experiments, we used the incorporation of labeled amino acids (AAs) as a proxy for heterotrophic activity and showed different levels of incorporation among different taxonomic groups. Taxon-specific differences in the net incorporation of AA-derived C and N indicate that the C/N relative use efficiency ranged from 0.8 to 1.4, where 1 reflects stoichiometric incorporation of C and N. Our results revealed that microbial organic matter processing is affected by taxon-specific physiological diversity, both in terms of general activity levels and in the ratio of assimilated C/N.

Introduction

In aquatic environments, bacteria process an average of 50% of phytoplankton primary production through the incorporation of dissolved organic matter (DOM; Giovannoni & Stingl, 2005). This bacteria-DOM coupling is highly variable in space and time, and the controls of this variability remain unclear (Azam *et al.*, 1993). Marine DOM is primarily composed of amino acids (AAs), amino sugars and neutral sugars (Kaiser & Benner, 2009). Considerable research, utilizing a variety of techniques and spanning three decades, has demonstrated that AAs are among the main sources of C and N for marine bacteria (Wheeler & Kirchman, 1986; Cottrell & Kirchman, 2000; Poretsky *et al.*, 2010). The standing pool of AAs is relatively low, typically from hundreds of nanomolar to the low micromolar range in eutrophic estuaries (Evens & Braven, 1988; Coffin, 1989). However, it is believed that AA turnover is quite fast due to high proteolytic activity measured in the bulk ocean (Smith *et al.*, 1992) or from individual marine bacterial isolates (Martinez *et al.*, 1996). The ubiquity of bacterial AA use is exemplified by the fact that one of the primary methods to calculate bacterial C demand in aquatic ecosystems involves measurement of radio-labeled leucine incorporation (Kirchman *et al.*, 1985). While the importance of AA incorporation by natural communities in response to C and N demand has been established by bulk methods (Jørgensen *et al.*, 1993; Kroer *et al.*, 1994), our ability to quantitate the relative rates C and N assimilation by distinct species has been impeded by methodological limitations. Such data would be helpful to understand how microbial community changes affect elemental cycling, in particular, the interplay between the cycles of C and N.

In the past decade, the stable isotope probing (SIP) approach (Radajewski *et al.*, 2000; Manefield *et al.*, 2002) has become one of the primary methodologies used to

FEMS MICROBIOLOGY ECOLOGY

link specific microbes with substrate utilization, particularly in complex communities. Conceptually, a dual ^{13}C and ^{15}N SIP experiment might be the ideal way to address the known interactions between C and N cycles (Hessen *et al.*, 2004) at the individual taxon level. While ^{13}C SIP has become part of the standard microbial ecology toolkit, ^{15}N SIP has been less widely applied (Wawrik *et al.*, 2009, 2012; Gallagher *et al.*, 2010; Andeer *et al.*, 2012) and is a more challenging procedure requiring at least 30 atm% ^{15}N enrichment for DNA or more for ^{15}N RNA SIP (Buckley *et al.*, 2007; Addison *et al.*, 2010). A new approach to SIP, Chip-SIP, circumvents some of the difficulties of separating ^{15}N DNA and RNA in a density gradient by separating microbial community RNA on a phylogenetic microarray for subsequent isotopic analysis with a Cameca NanoSIMS 50 (Cameca, Gennevilliers, France), an imaging secondary ion mass spectrometer (Mayali *et al.*, 2012).

In the present report, we applied Chip-SIP to a natural estuarine community to quantitate simultaneous C and N incorporation from dual-labeled substrates. First, we compared microarray RNA fluorescence from replicate incubations over time to determine the reproducibility of RNA hybridization patterns and how these patterns change temporally after incubation in bottles. This is relevant to the so-called bottle effect (Hammes *et al.*, 2010), that is, that enclosure of a volume of water in a container leads to changes in the microbial community over time. Concurrently, we examined $^{15}NH_4^+$ incorporation into RNA over the same time course to identify the appropriate temporal sampling necessary for successful label detection while minimizing bottle effects and trophic cross-feeding of labeled substrates, both of which would presumably increase with longer incubations. We subsequently investigated the taxon-specific incorporation patterns of labeled AAs in a different water sample collected at the same site to quantitate the relative activities of different taxa. From this same sample, we examined the simultaneous incorporation of both C and N from AAs by different taxa to test the hypothesis that different microbial groups from the same water sample incorporated different proportions of C/N from readily available organic substrates such as AAs. Such a result would identify one mechanism (taxon-specific physiological differences in C/N assimilation) to explain the general variability of bacterial DOM processing in aquatic ecosystems.

Materials and methods

Incubation of field samples

Surface water for all experiments was collected at the public pier in Berkeley, CA USA (37°51′46.67″N, 122°19′3.23″W) and brought back to the laboratory within 1 h in a cooler, after which incubation experiments were carried out. Glass bottles (700 mL) were filled initially without air space and dark incubated at 14 °C. For the first set of experiments, water samples were incubated in six bottles on 7/9/2009; three bottles were unamended and three amended with 200 μM 99 atm% ^{15}N ammonium. Each bottle was sampled after 2, 6, and 24 h by filtration of 100 mL through a 0.22 polycarbonate filter, which was then immediately frozen at − 80 °C. For the second set of experiments, a water sample collected on 10/15/2009 was incubated with 1 mg L^{-1} mixed AAs (99 atm% ^{13}C and 99 atm% ^{15}N labeled; Sigma; corresponds to 8 μM, on the high end of what has been measured in estuaries), collected by filtration after 12 h and frozen at − 80 °C.

RNA extraction and labeling

Total RNA from frozen filters was extracted with the Qiagen RNEasy kit according to manufacturer's instructions. RNA samples were split: one fraction saved for fluorescent labeling (see below), the other was unlabeled and stored for later NanoSIMS analysis. This procedure was used because the fluorescent labeling protocol introduces background (mostly ^{12}C and ^{14}N) that dilutes the ^{13}C and ^{15}N signal. Alexafluor 532 labeling was carried out with the Ulysis kit (Invitrogen) for 10 min at 90 °C (2 μL RNA, 10 μL labeling buffer, 2 μL Alexafluor reagent) followed by fragmentation. All RNA (fluorescently labeled or not) was fragmented using 1 × fragmentation buffer (Affymetrix) for 10 min at 90 °C before hybridization. Fluorescently labeled RNA was purified using a Spin-OUT^{TM} minicolumn (Millipore), and RNA was concentrated by isopropanol precipitation to a final concentration of 500 ng μL^{-1}.

Probe design

We designed 25 base DNA probes (Supporting Information, Table S1) specific for the 16S or 18S sequences of rRNA gene operational taxonomic units (OTU) using the Greengenes database (DeSantis *et al.*, 2006) implemented in the ARB software (Ludwig *et al.*, 2004). We designed 30 probes for each of 181 target taxa, minimizing cross-hybridization potential, as outlined previously (Mayali *et al.*, 2012). Targets included four domain or phylum-specific taxa for which probes could be designed (Bacteria, *Rhodobacteriaceae*, *Planctomycetes*, Marine Group A) as well as 177 more specific OTUs (Table S1). OTUs were not chosen based on specific 16S rRNA gene percent dissimilarity due to the uneven variability of 16S and 18S rRNA gene diversity among taxonomic groups.

Instead, OTUs were chosen based on monophyletic groups of sequences in the Greengenes database as implemented in ARB.

Microarray hybridization and NanoSIMS

Glass slides coated with indium-tin oxide (Sigma) were coated with silane Super Epoxy 2 (Arrayit Corporation) to provide a starting matrix for DNA synthesis. Microarrays (spot size = 17 μm) were synthesized using a photolabile deprotection strategy (Singh-Gasson *et al.*, 1999) on the LLNL Maskless Array Synthesizer (Roche Nimblegen, Madison, WI). Reagents for synthesis (Roche Nimblegen) were delivered through the Expedite (PerSeptive Biosystems) system. Similar arrays are available directly from Roche Nimblegen through special ordering. For array hybridization, RNA samples (1 μg) in 1 × Hybridization buffer (Roche Nimblegen) were placed in Nimblegen X4 mixer slides and incubated inside a Maui hybridization system (BioMicro® Systems) for 18 h at 42 °C and subsequently washed according to manufacturer's instructions (Roche Nimblegen). Arrays with fluorescently labeled RNA were imaged with a Genepix 4000B fluorescence scanner at pmt = 650 units. Slides were cut with a diamond pen and loaded into the NanoSIMS on a standard holder without coating.

Imaging secondary ion mass spectrometer analysis of microarrays hybridized with ^{13}C and/or ^{15}N enriched RNA was performed at LLNL with a Cameca NanoSIMS 50 (Cameca). Arrays were sputtered with a Cs^+ primary ion beam to generate negative secondary ions. Carbon and nitrogen isotopic ratios were determined by electrostatic peak switching on electron multipliers in pulse counting mode, alternately measuring $^{12}C^{14}N^-$ and $^{12}C^{15}N^-$ simultaneously for the $^{15}N/^{14}N$ ratio, and then measuring $^{12}C^{14}N^-$ and $^{13}C^{14}N^-$ simultaneously for the $^{13}C/^{12}C$ ratio. Additional details of the instrument parameters are provided elsewhere (Mayali *et al.*, 2012). Ion images were digitally stitched together and processed to generate isotopic ratios with custom software (LIMAGE, L. Nittler, Carnegie Institution of Washington). Isotopic ratios were converted to delta (permil) values using:

$$\delta = [(R_{meas}/R_{standard}) - 1] \times 1000, \quad (1)$$

where R_{meas} is the measured ratio, and $R_{standard}$ is the natural abundance standard ratio: 0.00367 for $^{15}N/^{14}N$ and 0.011237 for $^{13}C/^{12}C$ (Rundel *et al.*, 1989). Relative isotopic incorporation was quantified based on the hybridization-corrected enrichment (HCE), which is the slope of delta permil over fluorescence for a given set of probes (Mayali *et al.*, 2012).

Quantification of relative C and N incorporation and C/N relative use efficiency

We took two approaches to enable comparison of C and N incorporation from the dual-labeled AAs. First, we calculated a background-corrected atom percent excess (APE) to enable the direct comparison of ^{13}C and ^{15}N uptake by individual taxa. Then we calculated substrate utilization to account for ^{13}C incorporation relative to ^{15}N incorporation, which provides a metric for substrate use for C relative to N for each taxon. We define this ratio of relative substrate use as the C/N relative use efficiency.

APE is a metric for uptake of a rare isotope relative to the initial abundance of the rare isotope. It is defined as:

$$APE = [R_f/(R_f + 1) - R_i/(R_i + 1)] \times 100\%, \quad (2)$$

where R_f is the final ratio ($^{13}C/^{12}C$ or $^{15}N/^{14}N$), for which we use R_{meas} for the individual probe spots, and R_i is the initial ratio ($^{13}C/^{12}C$ or $^{15}N/^{14}N$), for which we use the average R_{meas} for unenriched probe spots, which reflects the initial community mean isotopic ratios and corrects for instrumental mass fractionation.

To correct for background N and C, we estimated the relative N and C background using previously published Chip-SIP data (Mayali *et al.*, 2012): we calculated APE values for single bacterial strains in that study grown through many generations in media with 100%, 50%, 10%, and 0.5% added ^{13}C and 25%, 10%, and 0.1% added ^{15}N. The APE data were plotted against fluorescence to calculate a slope for each culture (this is analogous to HCE which uses permil values, but uses APE instead). We graphed these slopes, which we call 'fluorescence-normalized APE', against the known isotopic enrichment values for both ^{15}N and ^{13}C labeled cultures (Fig. 1). These data showed that ^{15}N and ^{13}C did not follow the same relationship, but instead ^{15}N enrichment, as detected by Chip-SIP, was relatively higher, meaning that the C background on the arrays is higher than the N background. We calculated an APE_{15N}-to-APE_{13C} correction factor by taking the ratio of the two slopes, which yielded 1.7 ± 0.2 (1 standard error). This factor was divided into individual APE_{15N} measurements in this study to make relative APE values that enable direct comparison of C and N incorporation by taxon.

To determine whether C or N from a given substrate was incorporated preferentially by an individual taxon, we calculated the relative mass of the substrate needed to account for the C and N incorporation measured. Note that relative isotope incorporation and relative substrate use differ because the C/N ratio of the AAs and the microbial biomass differ (*c.* 4 vs. *c.* 6). Here, we assumed

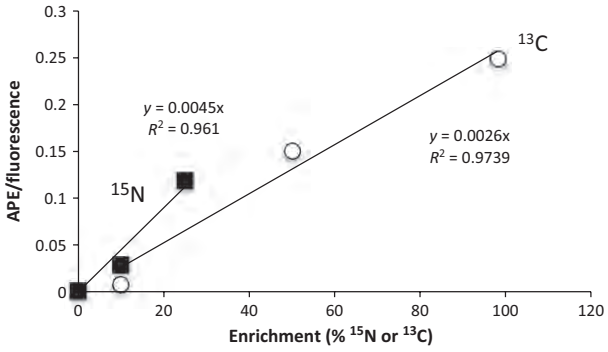

Fig. 1. Measurements of fluorescence-normalized APE for seven data sets of single bacterial strains grown on known ^{13}C or ^{15}N enriched media, including 100%, 50%, 10%, and 0.5% added ^{13}C and 25%, 10%, and 0.1% added ^{15}N. Each point represents the slope of APE over fluorescence for a probe set for a given concentration of added isotope.

a C/N value for AAs corresponding to the average of the 20 AAs (= 4.3 mol/mol), and the C/N of bacterial biomass to correspond to average measured values for coastal bacteria of 6 C to 1 N (Fukuda *et al.*, 1998). While there are possible mechanisms by which the rRNA in the microbes could differ in isotopic composition from the bulk microbe, here we assume that the isotopic composition of the rRNA-targeted by Chip-SIP is comparable to that of the organism as a whole and represents a good marker for correlating isotopic labeling and growth rate (MacGregor *et al.*, 2006).

The relative mass of substrate necessary to account for the C and N incorporation (and C/N relative use efficiency) is calculated using the net incorporation of each compared with the C and N content of the substrate. To derive this relative value, we start with the exact equation for net incorporation for C or N (Popa *et al.*, 2007):

$$F_{X_{net}} = \frac{R_f[1 - R_i/(R_i + 1)] - R_i/(R_i + 1)}{R_s/(R_s + 1) - R_f[R_s/(R_s + 1)]} \times 100\%, \quad (3)$$

where $F_{X_{net}}$ = net uptake for element X (C or N), R_f is the final isotopic ratio in the sampled biomass, and R_i and R_s are the isotopic ratios in the initial biomass and the substrate, respectively. R_f is calculated based on Eqn (2) and the APE_{15N}-to-APE_{13C} correction factor estimated above.

To get at the relative mass of substrate used for C or N, we write a general mass balance:

$$M_{s_X} \times F_{s_X} = M_{X_s}, \quad (4)$$

where M_{s_X} is the mass of the substrate needed to account for the net uptake of element X (C or N), F_{s_X} is the fraction of the substrate that is element X by mass, and M_{X_s} is the mass of element X taken up by the biomass. To establish a relationship between element source and the biomass, this mass balance can be compared with the mass balance for the biomass:

$$M_b \times F_{b_X} = M_{X_b}, \quad (5)$$

where M_b is the mass of the biomass, F_{b_X} is the fraction of the biomass that is element X by mass, and M_{X_b} is the mass of element X in the biomass. Note that the ratio of M_{s_X} to M_{X_b} is the net uptake of element X. Therefore, using the ratio of Eqns (4) and (5) we obtain:

$$(M_{s_x} \times F_{s_x})/(M_b \times F_{b_x}) = F_{X_{net}}. \quad (6)$$

To obtain the relative substrate incorporation for C and N, we divide Eqn (6) for C by the same equation for N:

$$\frac{(M_{s_C} \times F_{s_C})/(M_b \times F_{b_C})}{(M_{s_N} \times F_{s_N})/(M_b \times F_{b_N})} = \frac{F_{C_{net}}}{F_{N_{net}}}. \quad (7)$$

Note that F_{s_C}/F_{s_N} is equal to the C/N ratio for the substrate, and F_{b_C}/F_{b_N} is equal to the C/N ratio for the biomass. Therefore, this equation simplifies to:

$$\frac{M_{s_C}}{M_{s_N}} = \frac{F_{C_{net}} \times (C:N)_b}{F_{N_{net}} \times (C:N)_s}, \quad (8)$$

where M_{s_C}/M_{s_N} is the relative mass of the substrate necessary to account for the C incorporation from the substrate relative to N, which is the C/N relative use efficiency for the substrate.

Results

Reproducibility of community RNA hybridization

Our first set of incubations was in part designed to measure the reproducibility of community RNA hybridization patterns on a rRNA-targeted phylogenetic microarray. Each community RNA sample was hybridized to three replicate arrays within the same hybridization chamber, on the same slide, to determine whether physical location on the array surface affected hybridization patterns. Fluorescence patterns of replicate arrays within the same hybridization were reproducible, with pairwise linear regression analyses between replicate array data yielding R^2 values between 0.87 and 0.92 (Fig. S1). We then compared RNA fluorescence patterns from the original SF Bay water sample (T = 0 h) with those of the average of duplicate samples collected after incubation in bottles for 2, 6, and 24 h. As evidenced by decreasing R^2 values with increasing incubation time, samples incubated for 0 and 2 h were most similar to one another (R^2 = 0.88; Fig. 2a)

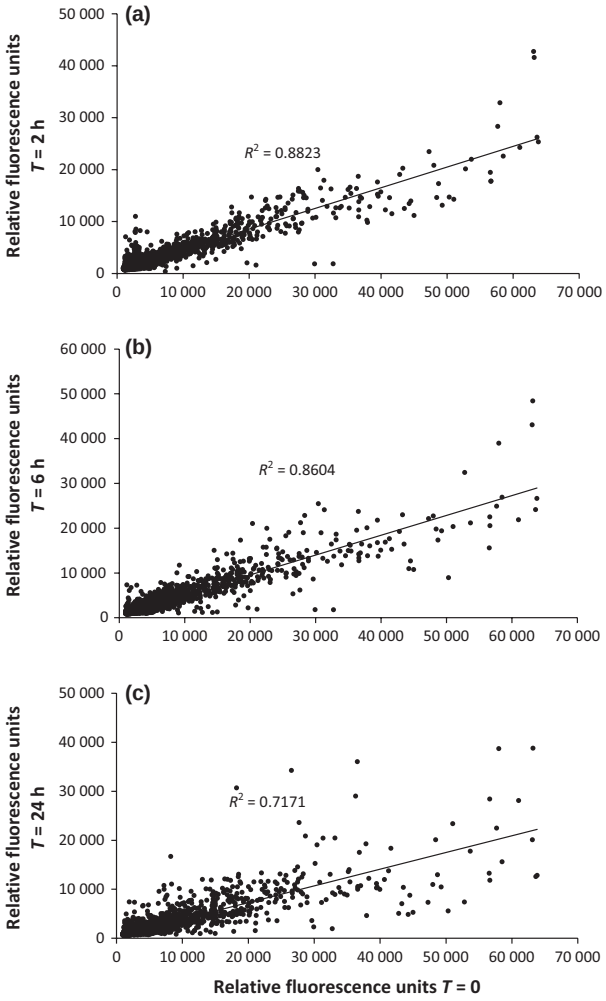

Fig. 2. Pairwise comparisons of probe fluorescence for RNA extracted from a seawater sample collected from SF Bay (T = 0 h) vs. the average of the same sample incubated in two bottles for T = 2 h (a), 6 h (b), or 24 h (c). Each point corresponds to an individual probe and is the average value from three replicate arrays (N = 5495).

followed by those incubated for 0 and 6 h (R^2 = 0.86; Fig. 2b), and those incubated for 0 and 24 h were least similar (R^2 = 0.72; Fig. 2c). We also examined which taxa changed in relative abundance after incubation in bottles for 6 and 24 h by calculating individual slopes for each taxon (Table S2).

Isotopic incorporation over time

In the first set of experiments, we concurrently incubated a second set of water samples with added $^{15}NH_4^+$ to determine the minimum incubation time needed for detectable isotope incorporation into RNA. We hybridized RNA from samples collected after 2, 6, or 24 h to the microarray described above, and NanoSIMS imaging was used to quantitate ^{15}N enrichment for the most abundant taxa. These abundant taxa were determined from the fluorescence signal, defined as rRNA OTUs with at least two probes having a signal > 3 times the background. The number of taxa analyzed by NanoSIMS was different for the three time points because rRNA OTU evenness based on RNA fluorescence decreased over time: we examined 30 taxa in the 2 h sample, 13 taxa in the 6 h sample, and 8 taxa in the 24 h sample. We considered a rRNA OTU isotopically enriched when at least two probes exhibited significant enrichment above background. The 2-h incubation sample exhibited little to no isotopic enrichment, with only 1 of 30 examined rRNA OTUs exhibiting isotopic enrichment. After 6 h, four of 13 OTUs were isotopically enriched, and after 24 h, all eight rRNA OTUs examined were isotopically enriched (data not shown). Based on these experiments, we determined that incubation for > 6 h was optimal for detectable isotopic enrichment from rRNA hybridized to the array. We further examined the temporal isotopic incorporation patterns of four rRNA OTUs with high fluorescence values at all three times points, representing three bacterial taxa (OTUs alpha1, bacter7, and betaOM43) and one eukaryote (OTU alveo4). The three bacterial taxa represent 16S rRNA gene phylotypes found to be abundant and widespread in the environment, as exemplified by the number of sequences in Genbank found with 99% or greater similarity to their representative sequences: 75 sequences for bacter7, 99 for alpha1, and 76 for betaOM43. OTU alpha1 is a member of the abundant *Roseobacter* NAC11-7 group (Yao *et al.*, 2011), betaOM43 of the abundant OM43 methylotrophic group (Giovannoni *et al.*, 2008), and bacter7 is a *Bacteroidetes* found in many marine samples, including at the San Pedro Channel Microbial Observatory, California (Fuhrman *et al.*, 2006). Measured isotopic enrichment for the four OTUs analyzed at all three time points were plotted against fluorescence (Fig. 3), demonstrating increasing incorporation of labeled ammonium over time. As reported previously (Mayali *et al.*, 2012), the level of probe hybridization, as measured by fluorescence, affected the absolute value of probe enrichment and must be accounted for when comparing the relative enrichment of different taxa. Of the four examples displayed in Fig. 3, the three bacterial taxa exhibited isotopic enrichment after 6 h, while the eukaryotic taxon did not show incorporation until the 24 h sample. This taxon had the second highest measured isotopic incorporation at the 24 h sample, suggesting it may have responded to the ammonium enrichment more slowly than the bacteria or, more likely, was a bacterivore that incorporated isotopic label via the ingestion of labeled bacteria.

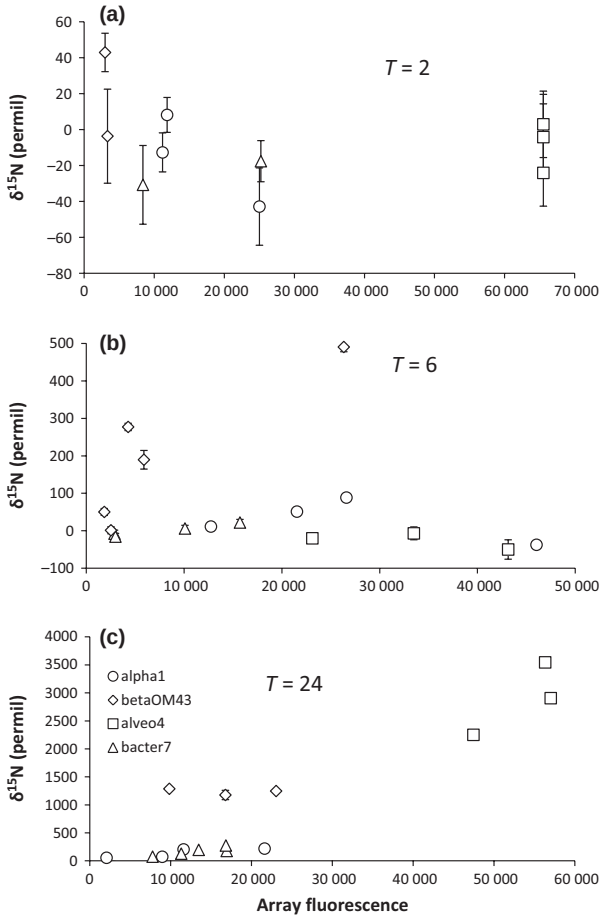

Fig. 3. Isotopic enrichment (in delta permil ^{15}N) plotted against fluorescence for 16S/18S probes targeting three bacterial (alpha1, bacter7, betaOM43) and one eukaryotic (alveo4) rRNA OTU following incubation with 200 μM $^{15}NH_4^+$ for 2 h (a), 6 h (b), and 24 h (c). Error bars correspond to standard error based on NanoSIMS count rate, and each point corresponds to an individual 25 bp probe spot. Note differences in *Y*-axis scale.

AA incorporation for activity measurements

As with many other identity function methods, the application of Chip-SIP to marine communities requires bottle incubations of water samples in the presence of added tracer substrates. These experiments must be closely monitored to limit the change in community composition and cross-feeding, where the metabolites of an isotopically labeled molecule are incorporated by secondary consumers. Our previous experiment with $^{15}NH_4^+$ additions suggested incubations lasting between 6 and 24 h would be suitable to detect isotopic incorporation while minimizing bottle effects (Hammes *et al.*, 2010) and cross-feeding of labeled substrates (Neufeld *et al.*, 2007). Therefore, we used a 12-h incubation period for our subsequent experiment with ^{15}N and ^{13}C labeled AAs. As

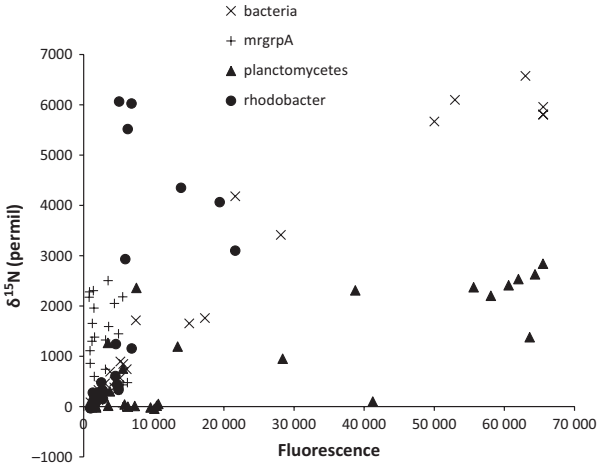

Fig. 4. Isotopic enrichment (in delta permil ^{15}N) plotted against fluorescence for four phylum or domain level taxa following incubation with labeled AAs after incubation for 12 h. Each point corresponds to an individual probe spot.

above, isotope incorporation results were graphed against fluorescence to allow relative comparisons among taxa. Initially focusing only on ^{15}N incorporation and broad taxa, we found that Marine Group A incorporated more ^{15}N from AAs, followed by *Rhodobacteriaceae*, the domain Bacteria, and the family *Planctomycetes* (Fig. 4). Data from these broad taxonomic groups as well as individual OTUs are reported with the slope of isotopic enrichment/fluorescence (= HCE; Table 1). The most enriched taxon was a eukaryote (OTU alveo5), followed by a member of the *Bacteroidetes* (OTU bacter7). Two targeted archaeal taxa (eurygrpII3 and eurygrpII10) exhibited no detectable isotopic enrichment from AAs (Table 1).

Comparison of ^{13}C and ^{15}N incorporation

In a final set of experiments, we tested the null hypothesis that the net C/N incorporation from AAs was constant among different microorganisms. We analyzed 10 taxa for which we previously collected ^{15}N data and examined the incorporation of both ^{13}C and ^{15}N, calculating relative APE values for each probe spot. Independent of probe spot taxonomic identity, ^{13}C and ^{15}N enrichment data were well correlated ($R^2 = 0.94$, $P < 0.0001$; Fig. 5a), though they did not correspond to the 1 : 1 line but rather were more enriched in ^{15}N, even after background correction. On an individual basis, some probe spots appeared to deviate from the average $^{13}C/^{15}N$ of incorporated AAs (e.g. the open squares, representing OTU bacter7, in Fig. 5a). To quantitate such differences, we calculated the C/N relative use efficiency for the substrate (AAs in this case) for each taxon, based on mass balance

Table 1. List of taxa analyzed by Chip-SIP after incubation with $^{15}NH_4^+$ and/or dual-labeled AAs. Probe sequences are provided in Table S1. HCE values for each organism were calculated using delta ^{15}N permil and fluorescence values for a probe set for samples incubated with AAs

Taxon	HCE	ARB SILVA taxonomy	Representative GB ACC#
alveo5	0.424	Eukarya/*Alveolates*/*Syndiniales*_Dino-Group I	EU780623
bacter7	0.2987	*Bacteroidetes*/*Flavobacteria*/*Cryomorphaceae*_Owenweeksia	AM279164
mrgrpA	0.2898	*Deferribacteres*/SAR406_Marine Group A	Phylum
rhodo	0.2556	*α-Proteobacteria*/*Rhodobacteriaceae*	Family
alpha1	0.2	*α-Proteobacteria*/*Rhodobacteriaceae*/*Roseobacter* NAC11-7	DQ009312
acido4	0.1386	*Acidobacteria*/*Holophagae*/TK85	EU491665
gamma4	0.1355	*γ-Proteobacteria*/*Alteromonadales*/SAR92	EF575231
gamma2	0.111	*γ-Proteobacteria*/*Oceanospirillales*_3/SAR86	EF574363
bacteria	0.1013	Bacteria	Domain
betaOM43	0.1002	*β-Proteobacteria*/*Methylophilales*/OM43	EU287057
gamma6	0.0921	*γ-Proteobacteria*/*Oceanospirillales*_3/ZD0405	DQ009424
verru4	0.0826	*Verrucomicrobia*/*Opitutae*/MC11C04 marine group	EU010231
gamma11	0.0805	*γ-Proteobacteria*/*Oceanospirillales*_*Oceanospirillaceae*	DQ009155
alveo4	0.0417	Eukarya/*Alveolates*/*Syndiniales*_Dino-Group I	DQ504313
plancto	0.0374	*Planctomycetes*	Phylum
alpha2	0.0323	*α-Proteobacteria*/*Rhodobacteriaceae*_1/uncultured	EF572888
eurygrpII3*	0.009	*Euryarchaeota*/*Thermoplasmatales*/Marine Group II	AB629532
alpha23*	− 0.0005	*α-Proteobacteria*/*Rickettsiales*/SAR116	AY907748
eurygrpII10*	− 0.0164	*Euryarchaeota*/*Thermoplasmatales*/Marine Group II	AB301902

GB acc#, Genbank accession number.
*HCE values not significantly greater than zero, meaning that isotopic incorporation was not confirmed.

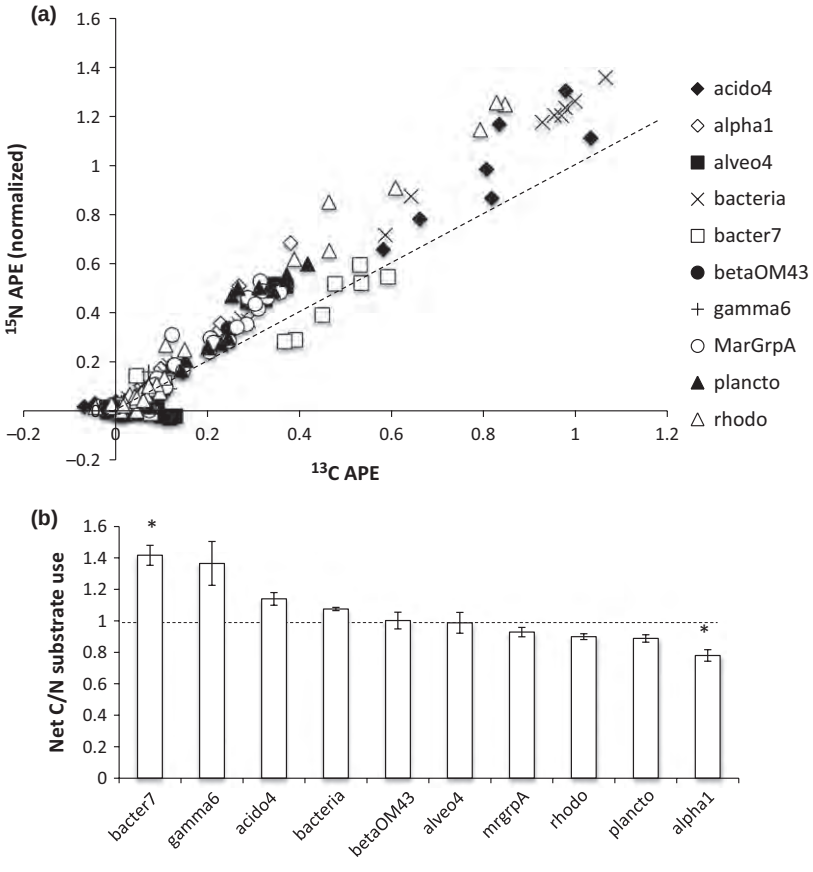

Fig. 5. (a) Comparison of ^{13}C and ^{15}N isotopic enrichment (in APE, normalized for array background) for marine microbial taxa after incubation with dual-labeled AAs for 12 h; dotted line represents equal ^{13}C and ^{15}N enrichment of the probe spots, but not equal C/N incorporation from the substrate. (b) taxon-specific net C/N incorporation from the substrate, based on mass balance calculations, and taking into account, the C/N of both the substrate and the biomass (error bars = 1 standard error). The dotted line represents equivalent ^{13}C and ^{15}N incorporation from the substrate, and * denoted taxa with C/N relative substrate use from AAs significantly different from 1.

calculations taking into account the C/N ratio of both the AAs and the biomass (see equations in the Materials and methods). C/N relative use efficiency for AAs ranged from 0.8 to 1.4 (Fig. 5b). The C/N relative use efficiency for two of 10 taxa were statistically different from 1 based on a Tukey HSD test, where 1 means C and N were incorporated from the AAs in stoichiometric amounts. We realize that more statistical power would likely increase the number of taxa with C/N relative use efficiencies significantly different than 1, but for ease of discussion, we divided taxa into those with stoichiometric C/N use, those that incorporated more C than N, and those that incorporated more N than C. OTU bacter7 (a *Bacteroidetes*) exhibited 40% higher C use efficiency than N and OTU alpha1 (a *Roseobacter*) exhibited 25% higher N use efficiency than C.

Discussion

RNA hybridization for microbial community fingerprinting

The Chip-SIP approach relies on hybridization of 16S rRNA gene without PCR amplification because nucleic acid amplification would remove any isotopic enrichment signal. We have previously shown that this approach can detect at least 10 ng from a single strain, corresponding to 1% of the community (Mayali *et al.*, 2012). Here, we showed that microarrays that target ribosomal RNA were reproducible and their use is a suitable approach to compare microbial communities from different samples. As expected, as seawater was incubated for longer periods of time (2, 6, 24 h), its microbial community fingerprints (measured by RNA hybridization patterns) increasingly diverged from the original sample (Fig. 2). These results are consistent with a previous study documenting microbial community shifts in 24-h bottle incubations of seawater (Agis *et al.*, 2007). Not surprisingly, we conclude that longer incubations will lead to some changes in microbial community composition, and thus bottle incubation time should be minimized as much as possible.

Concurrent with the microbial community composition analyses by rRNA hybridization fluorescence patterns, we also examined isotopic incorporation over time, using $^{15}NH_4^+$ as a substrate. The ultimate goal of these experiments was to optimize incubation times to achieve detectable isotopic incorporation while minimizing changes in microbial community structure. We found nearly undetectable isotopic incorporation after 2 h, relatively low incorporation after 6 h, and ample incorporation after 24 h. With the knowledge that microbial community structure changes increase with increasing incubations time, we chose an intermediate incubation time of 12 h (between 6 and 24 h) for all subsequent experiments. While this timeframe is significantly longer than incubations for bacterial carbon production using leucine (Kirchman *et al.*, 1985), it is less than most SIP experiments carried out with samples from soil and sediment (Murrell & Whiteley, 2010) and the few carried out with samples from the marine environment (Neufeld *et al.*, 2008; Wawrik *et al.*, 2009, 2012; Redmond & Valentine, 2011).

AA incorporation to measure taxon-specific activity

There is no standard methodology to quantitate the activity of bacteria (and other heterotrophs) in aquatic samples. Strategies include the use of redox-sensitive dyes to measure respiring cells (Rodriguez *et al.*, 1992), flow-cytometric analysis of cells with high nucleic acid content (Gasol *et al.*, 1999), and incubation with labeled thymidine (Fuhrman & Azam, 1980) or leucine (Kirchman *et al.*, 1985), either in bulk or in combination with fluorescent *in situ* hybridization and microautoradiography (Ouverney & Fuhrman, 2000). In a previous study, the incorporation of mixed AAs was correlated with detection using universal rRNA-targeted probes (Karner & Fuhrman, 1997), suggesting that the use of AAs as substrates is a good proxy to detect active cells with high ribosomal content. Furthermore, environmental transcriptomics suggests that all major marine bacterial taxa express AA transporters (Poretsky *et al.*, 2010). Therefore, we used the incorporation of ^{15}N from stable isotope labeled AAs as a proxy for microbial activity.

Our results from the AA incubations revealed distinct incorporation patterns based on taxonomy (Fig. 4, Table 1). These patterns were apparent at different levels of phylogenetic resolution. At coarse resolution (e.g. phylum level or higher), the Marine Group A and the *Rhodobacteriaceae* were more isotopically enriched, and the *Planctomycetes* were less enriched, than more general probes targeting the domain Bacteria (Fig. 4). As the three groups belong to this domain, it was consistent that the bacterial isotopic enrichment data were intermediate as they represent the average enrichment for a highly diverse group comprised of taxa with both higher and lower enrichment. Patterns could be further broken down at the OTU level (Table 1), where the highest enrichment comprised a eukaryotic and a *Bacteroidetes* taxon. We also detected hybridized RNA from two Group II *Euryarchaeota* OTUs, both of which were not significantly enriched in ^{15}N. We conclude that these organisms were either (1) active but not incorporating AAs; (2) not active (either dead or dormant); or (3) incorporated AAs but not enough to detect. Although we

cannot reject any of these hypotheses, previous work suggests Chip-SIP is sensitive to low levels of isotopic incorporation such as 0.1% added ^{15}N (Mayali *et al.*, 2012). While incubations longer than 12 h might have led to detectable isotopic incorporation by those taxa, risks of substrate cross-feeding and increased changes in the microbial community structure would escalate. Like other SIP methods, Chip-SIP is able to identify the taxa that are most actively using a substrate, but it is not able to preclude low-level utilization. We also point out that because our detection limit is generally more sensitive than traditional SIP, we are able to detect isotopic incorporation in taxa with very little enrichment, which in theory could be from slow-growing or from cross-feeding organisms. Considering the turnover time of aquatic bacteria ranges from several days to weeks (Bell & Albright, 1982), it is more likely that we are detecting slower-growing organisms.

C and N incorporation from AAs

The proportion of bacterial C and N demand that is accounted for by AAs is dependent on multiple environmental factors, in particular the availability and the C/N ratio of other organic substrates (Goldman & Dennett, 1991). In addition, variability in bacterial growth efficiency and differences in N remineralization likely cause changes in the C/N incorporated into biomass. The variability of organic matter C/N incorporation patterns has not been investigated with modern molecular techniques, but was studied almost two decades ago using bulk methods. Jørgensen *et al.* (1993) found that the incorporation of AAs accounted for an average of 77% and 81% of net bacterial C and N production (i.e. net incorporation of new C and N), respectively. In an estuary, Kroer *et al.* (1994) showed that AAs provided 6–24% and 2–7% of the bacterial N and C demand (incorporation + remineralization), respectively. Using the bulk data from Jørgensen *et al.*, we calculate the average net C/N incorporation to be 0.95 (77/81) and the C/N relative use efficiency from AAs to be 1.36, which implies net remineralization of N. In our samples, the Chip-SIP data revealed that one bacterial OTUs (bacter7) exhibited similar C/N relative use efficiency. However, most taxa incorporated C and N from AAs stochiometrically (i.e. without preference, incorporating all of the C and the N from the AAs), and still one other incorporated more of the AA N than C.

Differences in C and N assimilation from AAs, assuming that the isotopic composition of the extracted RNA allows relative comparisons among taxa (MacGregor *et al.*, 2006) will be influenced by the combination of N remineralization from AAs and C respiration to CO_2 from AA breakdown. In other words, OTUs such as alpha1 (a *Roseobacter*) may have higher respiration rates than average (and lose more C from AAs) and/or have comparatively lower rates of N remineralization from AAs, which could be associated with decreased incorporation of other N molecules and/or increased incorporation of other C molecules. Conversely, rRNA OTUs such as bacter7 may have lower respiration rates, higher N remineralization rates, increased incorporation of other N molecules, and/or decreased incorporation of other C molecules. Members of the *Roseobacters* (Buchan *et al.*, 2005) and *Bacteroidetes* (Kirchman, 2002) are both known to be abundant in marine waters, particularly in association with algal blooms, but are believed to exhibit some general physiological differences. *Bacteroidetes* are thought to be major degraders of high molecular weight organic matter (Cottrell & Kirchman, 2000), whereas *Roseobacters* are hypothesized to be fast growing generalists for many substrates (Newton *et al.*, 2010). Our AA incorporation data suggest that they also exhibit different patterns of C/N relative use efficiency from AAs, with *Roseobacters* incorporating relatively more N and *Bacteroidetes* relatively more C. Assuming similar demands for C and N, it is possible that *Bacteroidetes* are using other N sources for its N demand. To test this hypothesis, we can compare $^{15}NH_4^+$ incorporation for these two taxa from our ammonium incorporation experiments (Fig. 3). These experiments, however, did not show a statistically significant difference in $^{15}NH_4^+$ incorporation. An alternative mechanism to explain differences in C/N relative use efficiency is that different taxa preferentially incorporated certain AAs over others. This has been documented with bulk methods (Barvenik & Malloy, 1979), and since each AA has a different C/N (range = 2–9), preferential uptake of some AAs over others would lead to our findings. While the mechanisms that resulted in the observed patterns are not identified, our results illustrate the species-specific physiological diversity that can exist among co-occurring microbes competing for the same resources.

Conclusion

Using a relatively new methodology, we have uncovered variability in the C/N incorporated by surface marine microorganisms from isotopically labeled mixed AAs. Our Chip-SIP analyses provide evidence to support the idea that the well-characterized high microbial diversity on the species level (Rappé *et al.*, 1997), as well as the genomic level (DeLong *et al.*, 2006), results in functional differences that we can measure in natural communities. Further, our data exemplify how the simultaneous analysis of taxon-specific ^{15}N and ^{13}C incorporation can provide quantitative measurements of biogeochemical

activity without cultivation. The use of this and other methods that combine molecular data with biogeochemical measurements will be crucial to test hypotheses about microbial control of C and N cycles in the environment.

Acknowledgements

We thank S. Mabery for technical support and L. Nittler for software development. The DOE Genomic Sciences Program (grant # SCW1039) and LLNL Laboratory Directed Research Development (LDRD) funding (grant # 11-ERD-066) supported this research. Work was performed under the auspices of the U.S. Department of Energy at Lawrence Livermore National Laboratory under Contract DE-AC52-07NA27344.

References

Addison SL, McDonald IR & Lloyd-Jones G (2010) Stable isotope probing: technical considerations when resolving ^{15}N-labeled RNA in gradients. *J Microbiol Methods* **80**: 70–75.

Agis M, Granda A & Dolan JR (2007) A cautionary note: examples of possible microbial community dynamics in dilution grazing experiments. *J Exp Mar Biol Ecol* **341**: 176–183.

Andeer P, Strand SE & Stahl DA (2012) High-sensitivity stable-isotope probing by a quantitative terminal restriction fragment length polymorphism protocol. *Appl Environ Microbiol* **78**: 163–169.

Azam F, Smith DC, Steward GF & Hagström Å (1993) Bacteria-organic matter coupling and its significance for oceanic carbon cycling. *Microb Ecol* **28**: 167–179.

Barvenik FW & Malloy SC (1979) Kinetic patterns of microbial amino acid uptake and mineralization in marine waters. *Estuar Coast Mar Sci* **8**: 241–250.

Bell CR & Albright LJ (1982) Attached and free-floating bacteria in a diverse selection of water bodies. *Appl Environ Microbiol* **43**: 1227–1237.

Buchan A, Gonzàlez JM & Moran MA (2005) Overview of the marine *Roseobacter* lineage. *Appl Environ Microbiol* **71**: 5665–5677.

Buckley DH, Huangyutitham V, Hsu S-F & Nelson TA (2007) Stable isotope probing with ^{15}N achieved by disentangling the effects of genome G + C content and isotope enrichment on DNA density. *Appl Environ Microbiol* **73**: 3189–3195.

Coffin RB (1989) Bacterial uptake of dissolved free and combined amino acids in estuarine water. *Limnol Oceanogr* **34**: 531–542.

Cottrell MT & Kirchman DL (2000) Natural assemblages of marine Proteobacteria and members of the Cytophaga-Flavobacter cluster consuming low- and high-molecular-weight dissolved organic matter. *Appl Environ Microbiol* **66**: 1692–1697.

DeLong EF, Preston CM, Mincer T *et al.* (2006) Community genomics among stratified microbial assemblages in the ocean's Interior. *Science* **311**: 496–503.

DeSantis TZ, Hugenholtz P, Larsen N, Rojas M, Brodie EL, Keller K, Huber T, Dalevi D, Hu P & Andersen GL (2006) Greengenes, a chimera-checked 16S rRNA gene database and workbench compatible with ARB. *Appl Environ Microbiol* **72**: 5069–5072.

Evens R & Braven J (1988) A seasonal comparison of the dissolved free amino acid levels in estuarine and English Channel waters. *Sci Total Environ* **76**: 69–78.

Fuhrman JA & Azam F (1980) Bacterioplankton secondary production estimates for coastal waters of British Columbia, Canada, Antarctica, and California, USA. *Appl Environ Microbiol* **39**: 1085–1095.

Fuhrman JA, Hewson I, Schwalbach MS, Steele JA, Brown MV & Naeem S (2006) Annually reoccurring bacterial communities are predictable from ocean conditions. *P Natl Acad Sci USA* **103**: 13104–13109.

Fukuda R, Ogawa H, Nagata T & Koike I (1998) Direct determination of carbon and nitrogen contents of natural bacterial assemblages in marine environments. *Appl Environ Microbiol* **64**: 3352–3358.

Gallagher EM, Young LY, McGuinness LM & Kerkhof LJ (2010) Detection of 2,4,6-trinitrotoluene-utilizing anaerobic bacteria by ^{15}N and ^{13}C incorporation. *Appl Environ Microbiol* **76**: 1695–1698.

Gasol JM, Zweifel UL, Peters F, Fuhrman JA & Hagstöm Å (1999) Significance of size and nucleic acid content heterogeneity as measured by flow cytometry in natural planktonic bacteria. *Appl Environ Microbiol* **65**: 4475–4483.

Giovannoni SJ & Stingl U (2005) Molecular diversity and ecology of microbial plankton. *Nature* **437**: 343–348.

Giovannoni SJ, Hayakawa DH, Tripp HJ *et al.* (2008) The small genome of an abundant coastal ocean methylotroph. *Environ Microbiol* **10**: 1771–1782.

Goldman JC & Dennett MR (1991) Ammonium regeneration and carbon utilization by marine bacteria grown on mixed substrates. *Mar Biol* **109**: 369–378.

Hammes F, Vital M & Egli T (2010) Critical evaluation of the volumetric "bottle effect" on microbial batch growth. *Appl Environ Microbiol* **76**: 1278–1281.

Hessen DO, Ågren GI, Anderson TR, Elser JJ & de Ruiter PC (2004) Carbon sequestration in ecosystems: the role of stoichiometry. *Ecology* **85**: 1179–1192.

Jørgensen NOG, Kroer N, Coffin RB, Yang X-H & Lee C (1993) Dissolved free amino acids, combined amino acids, and DNA as sources of carbon and nitrogen to marine bacteria. *Mar Ecol Prog Ser* **98**: 135–148.

Kaiser K & Benner R (2009) Biochemical composition and size distribution of organic matter at the Pacific and Atlantic time-series stations. *Mar Chem* **113**: 63–77.

Karner M & Fuhrman JA (1997) Determination of active marine bacterioplankton: a comparison of universal 16S rRNA probes, autoradiography, and nucleoid staining. *Appl Environ Microbiol* **63**: 1208–1213.

Kirchman DL (2002) The ecology of *Cytophaga-Flavobacteria* in aquatic environments. *FEMS Microbiol Ecol* **39**: 91–100.

Kirchman D, K'nees E & Hodson R (1985) Leucine incorporation and its potential as a measure of protein synthesis by bacteria in natural aquatic systems. *Appl Environ Microbiol* **49**: 599–607.

Kroer N, Jørgensen NOG & Coffin RB (1994) Utilization of dissolved nitrogen by heterotrophic bacterioplankton: a comparison of three ecosystems. *Appl Environ Microbiol* **60**: 4116–4123.

Ludwig W, Strunk O, Westram R *et al.* (2004) ARB: a software environment for sequence data. *Nucleic Acids Res* **32**: 1363–1371.

MacGregor BJ, Boschker HTS & Amann R (2006) Comparison of rRNA and polar-lipid-derived fatty acid biomarkers for assessment of ^{13}C-substrate incorporation by microorganisms in marine sediments. *Appl Environ Microbiol* **72**: 5246–5253.

Manefield M, Whiteley AS, Griffiths RI & Bailey MJ (2002) RNA stable isotope probing, a novel means of linking microbial community function to phylogeny. *Appl Environ Microbiol* **68**: 5367–5373.

Martinez J, Smith DC, Steward GF & Azam F (1996) Variability in ectohydrolytic enzyme activities of pelagic marine bacteria and its significance for substrate processing in the sea. *Aquat Microb Ecol* **10**: 223–230.

Mayali X, Weber PK, Brodie EL, Mabery S, Hoeprich P & Pett-Ridge J (2012) High-throughput isotopic analysis of RNA microarrays to quantify microbial resource use. *ISME J* **6**: 1210–1221.

Murrell JC & Whiteley AS (2010) *Stable Isotope Probing and Related Technologies*. ASM Press, Washington DC.

Neufeld J, Wagner M & Murrell J (2007) Who eats what, where and when? Isotope-labelling experiments are coming of age. *ISME J* **1**: 103–110.

Neufeld JD, Boden R, Moussard H, Schäfer H & Murrell JC (2008) Substrate-specific clades of active marine methylotrophs associated with a phytoplankton bloom in a temperate coastal environment. *Appl Environ Microbiol* **74**: 7321–7328.

Newton RJ, Griffin LE, Bowles KM *et al.* (2010) Genome characteristics of a generalist marine bacterial lineage. *ISME J* **4**: 784–798.

Ouverney CC & Fuhrman JA (2000) Marine planktonic archaea take up amino acids. *Appl Environ Microbiol* **66**: 4829–4833.

Popa R, Weber PK, Pett-Ridge J *et al.* (2007) Carbon and nitrogen fixation and metabolite exchange in and between individual cells of *Anabaena oscillarioides*. *ISME J* **1**: 354–360.

Poretsky RS, Sun S, Mou X & Moran MA (2010) Transporter genes expressed by coastal bacterioplankton in response to dissolved organic carbon. *Environ Microbiol* **12**: 616–627.

Radajewski S, Ineson P, Parekh NR & Murrell JC (2000) Stable-isotope probing as a tool in microbial ecology. *Nature* **403**: 646–649.

Rappé MS, Kemp PF & Giovannoni SJ (1997) Phylogenetic diversity of marine coastal picoplankton 16S rRNA genes cloned from the continental shelf off Cape Hatteras, North Carolina. *Limnol Oceanogr* **42**: 811–826.

Redmond MC & Valentine DL (2011) Natural gas and temperature structured a microbial community response to the Deepwater Horizon oil spill. *P Natl Acad Sci USA*, doi: 10.1073/pnas.1108756108.

Rodriguez GG, Phipps D, Ishiguro K & Ridgway HF (1992) Use of a fluorescent redox probe for direct visualization of actively respiring bacteria. *Appl Environ Microbiol* **58**: 1801–1808.

Rundel PW, Ehleringer JR & Nagy KA (1989) *Stable Isotopes in Ecological Research*. Springer Verlag, New York, NY.

Singh-Gasson S, Green RD, Yue Y, Nelson C, Blattner F, Sussman MR & Cerrina F (1999) Maskless fabrication of light-directed oligonucleotide microarrays using a digital micromirror array. *Nat Biotechnol* **17**: 974–978.

Smith DC, Simon M, Alldredge AL & Azam F (1992) Intense hydrolytic enzyme activity on marine aggregates and implications for rapid particle dissolution. *Nature* **359**: 139–142.

Wawrik B, Callaghan AV & Bronk DA (2009) Use of inorganic and organic nitrogen by *Synechococcus* spp. and diatoms on the West Florida shelf as measured using stable isotope probing. *Appl Environ Microbiol* **75**: 6662–6670.

Wawrik B, Boling WB, Van Nostrand JD, Xie J, Zhou J & Bronk DA (2012) Assimilatory nitrate utilization by bacteria on the West Florida Shelf as determined by stable isotope probing and functional microarray analysis. *FEMS Microbiol Ecol* **79**: 400–411.

Wheeler PA & Kirchman DL (1986) Utilization of inorganic and organic nitrogen by bacteria in marine systems. *Limnol Oceanogr* **31**: 998–1009.

Yao D, Buchan A & Suzuki MT (2011) *In situ* activity of NAC11-7 roseobacters in coastal waters off the Chesapeake Bay based on *ftsZ* expression. *Environ Microbiol* **13**: 1032–1041.

Supporting Information

Additional Supporting Information may be found in the online version of this article:

Fig. S1. Pairwise comparisons of probe fluorescence after hybridization to replicate array probe sets for RNA extracted from a seawater sample collected from SF Bay (a–c) and subsequently incubated in bottles for 2 h (d–f).
Table S1. List of probes targeting marine microbial taxa.
Table S2. Comparison of relative fluorescence units between the original SF Bay water sample with samples incubated for 6 and 24 h in glass bottles.

Please note: Wiley-Blackwell is not responsible for the content or functionality of any supporting materials supplied by the authors. Any queries (other than missing material) should be directed to the corresponding author for the article.